(Preprint) AAS 15-083

GLOBAL PRECIPITATION MEASUREMENT MISSION LAUNCH AND COMMISSIONING

Nikesha Davis*, Keith DeWeese*, Melissa Vess*, James R. O'Donnell, Jr., Ph.D.*, and Gary Welter†

During launch and early operation of the Global Precipitation Measurement (GPM) Mission, the Guidance, Navigation, and Control (GN&C) analysis team encountered four main on-orbit anomalies. These include: (1) unexpected shock from Solar Array deployment, (2) momentum buildup from the Magnetic Torquer Bars (MTBs) phasing errors, (3) transition into Safehold due to albedo induced Course Sun Sensor (CSS) anomaly, and (4) a flight software error that could cause a Safehold transition due to a Star Tracker occultation. This paper will discuss ways GN&C engineers identified the anomalies and tracked down the root causes. Flight data and GN&C on-board models will be shown to illustrate how each of these anomalies were investigated and mitigated before causing any harm to the spacecraft. On May 29, 2014, GPM was handed over to the Mission Flight Operations Team after a successful commissioning period. Currently, GPM is operating nominally on orbit, collecting meaningful scientific data that will significantly improve our understanding of the Earth's climate and water cycle.

INTRODUCTION

On February 27, 2014, the Global Precipitation Measurement (GPM) core observatory launched on a Japanese H-IIA launch vehicle from Tanegashima Space Center, located on the Japanese island of Tanegashima, Japan. GPM is an international partnership mission designed to help understand global precipitation and its effects on humankind. NASA Goddard Space Flight Center (GSFC) developed this project with the Japan Aerospace Exploration Agency. GPM core is part of an international constellation of Earth Science missions that will aid in improving the understanding of global precipitation and the Earth's water cycle. With the addition of GPM, these satellites gather global information on rain, snow, ice, and other global weather phenomena approximately every three hours. Scientists are able to use GPM data to help advance our understanding of Earth's water and energy cycles, improve the forecasting of extreme events that cause natural disasters, and extend current capabilities of using satellite precipitation information to directly benefit society.

GPM is a Low-Earth orbiting, nadir pointing satellite flying at an altitude of 400km with a 65° orbital inclination. The GPM spacecraft was designed for a three-year mission, with controlled reentry planned at end of life. It is equipped with two science instruments: the GPM Microwave Imager (GMI) and the Dual-Frequency Precipitation Radar (DPR) system. The GMI is a microwave radiometer, and the DPR is a precipitation radar system, consisting of Ku and Ka band radars. Data from these instruments are combined to provide three-dimensional precipitation observations, as

* Engineer, Attitude Control Systems Engineering Branch, NASA Goddard Space Flight Center, Greenbelt, MD
† Engineer, Flight Software Systems Branch, NASA Goddard Space Flight Center, Greenbelt MD.

well as an accurate rainfall rate. In order to give meaningful information, these instruments require precise pointing control with knowledge of 2.8 arcmin, 3-sigma about each axis. The GPM Guidance, Navigation, and Control (GN&C) system is responsible for controlling spacecraft attitude during nominal operations, orienting the spacecraft during instrument calibration maneuvers, commanding the solar arrays (SA) and high-gain antenna (HGA), controlling the spacecraft propulsion system for orbit maintenance and controlled reentry, and for spacecraft system momentum management. Figure 1 provides an image of GPM with the body coordinate system axes. Here, the GMI, DPR, HGA and two SA's are identified.

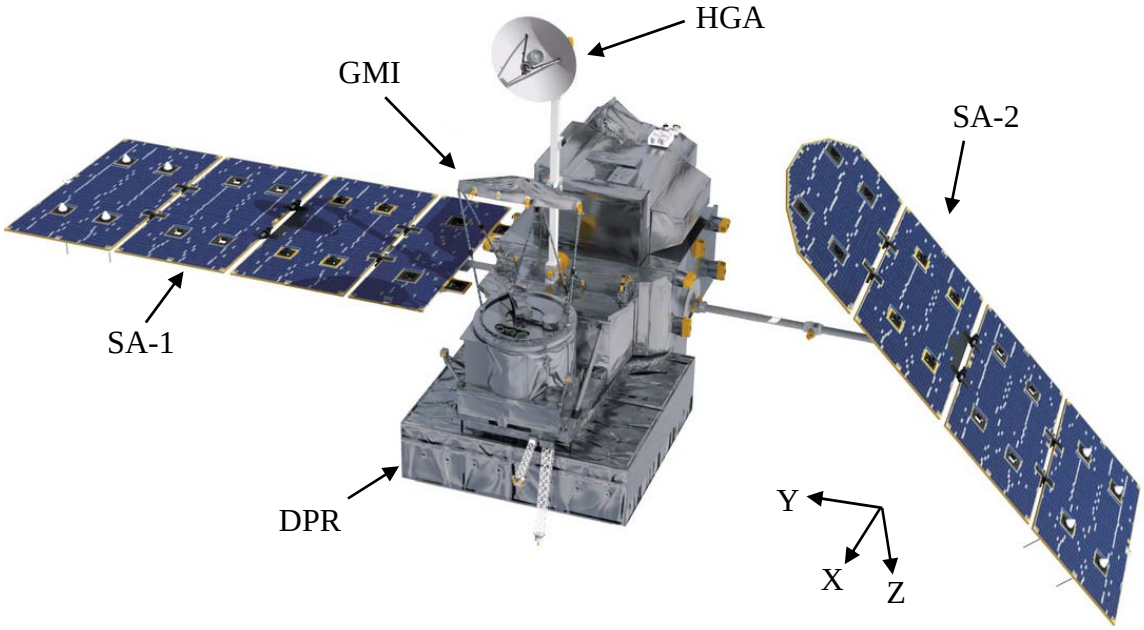

Figure 1: Diagram of GPM.

To ensure accurate control of the spacecraft and science instruments, GPM is equipped with a number of on-board sensors and actuators. These sensors include a Northrup Grumman Scalable Space Inertial Reference Unit (SSIRU), 24 Adcole Coarse Sun Sensors (CSSs), 2 Medium Sun Sensors (MSSs) each composed of 2 Adcole Coarse Analog Sun Sensors [1], 2 Macintyre Electronic Design Associates Three-Axis Magnetometers (TAMs), 2 Selex Galileo Star Trackers (STs), 2 in-house designed and built GSFC Navigator Global Positioning System (GPS) Receivers[2], and an optical encoder for each of the 4 SA/HGA gimbals. The actuator suite consists of 5 in-house designed and built GSFC Demiseable Integrated Reaction Wheel Assemblies (RWAs), 12 Aerojet 22-Newton thrusters, 3 dual-winding Goodrich Space Systems Torque Rods (Magnetic Torquer Bars, MTBs), and the GSFC dual wound SA/HGA gimbal motors. For the most part, these sensors and actuators were divided into the A-side and B-side of the spacecraft.

The GN&C subsystem is composed of six different control modes, each of which uses different combinations of the on-board actuators and sensors to ensure the spacecraft is in the safe and stable orientation needed to accomplish each controller's goal. The six control modes, most of which will be discussed in the course of the timeline below, are Rate Null, Sun Point, Slew, Delta H, Delta V, and Mission Science Modes. Mission Science Mode (MSM) is the control mode used for collecting science data. A number of constraints were taken into account when designing this control mode. For example, due to thermal constraints, the Sun is typically kept on the –Y side of the spacecraft. Additionally, the spacecraft nominally flies with a 4° pitch about the Y body axis in order to ensure

the body-fixed flight coordinate reference frame is in line with the Geodetic coordinate reference frame.

To ensure success of the science mission, GPM was designed to be single fault tolerant. In the event of any hardware or performance issue, a fault/failure detection feature was designed to autonomously ensure spacecraft safety, thus adhering to the NASA Reliability, Redundancy and Fault Tolerance safety design requirements. This Fault Detection and Correction (FDC) system compares spacecraft performance with "nominal" expectations. In cases where the spacecraft is not performing as expected, FDC will flag this behavior and start a sequence to safe the spacecraft until engineers can determine what corrective action(s) to take. When an FDC flag trips, it triggers an Action Point (AP). Each AP, when triggered, will start a Relative Time Sequence (RTS), which ultimately changes the configuration of the spacecraft based on predetermined safing precautions. This system is intended to confirm the spacecraft hardware is performing as expected, ensuring that the satellite stays in a safe and stable configuration. A number of the following anomalies caused an FDC trip.

POST-LAUNCH TIMELINE AND FLIGHT ANOMALIES

The GPM satellite was launched February 27th, Greenwich Mean Time (GMT) 058/18:37 on a Japanese H-IIA rocket. Launch configuration for GPM included the RWAs, STs, and GPS receivers off, while the IRUs and both Analog & Torquer Bar (ATB) command cards were powered on. As a result, prior to launch and separation, GN&C engineers were mostly monitoring the gyro rates. Approximately 10 minutes after liftoff, GMT 058/18:47, GN&C engineers started receiving data from the spacecraft. Post separation, the GN&C subsystem had a requirement to null spacecraft vehicle rates within 30 minutes using the 5 RWAs if the initial tip-off rates were less than ± [0.5, 1.0, 1.0] deg/sec. A little over 6 minutes after receiving data from the spacecraft, GMT 18:53, fairing separation was detected. The satellite was released from the launch vehicle with low residual spacecraft body rates of [0.004, 0.019, -0.039] deg/sec about the [x, y, z] axes, respectively. At this point, the RWAs were autonomously powered and the spacecraft transitioned into Rate Null Mode to remove any rate errors. These residual rates were removed in less than 20 seconds. Subsequently, the spacecraft transitioned to Sun Point Mode (SPM), and proceeded to acquire its Sun-pointing attitude. After switching to SPM, engineers began the process of early checkout activities for GPM.

For this satellite, early checkout included powering and verification of all on-board hardware systems. SA deployment began autonomously at GMT 058/19:03, approximately 10 minutes after separation. The first anomaly was detected at this time. It is discussed in detail in the section entitled 'Flight Anomaly 1.' During SA deployment, an FDC flag was triggered, causing the spacecraft to autonomously switch to Safehold on the B-side. In the GPM design, Safehold was considered a spacecraft state; the attitude control system mode used during Safehold is SPM. Once the root cause was understood, GN&C engineers sent the command to swap back to the A-side, since all the autonomous FDC was designed assuming the A-side was in control.

Shortly after the sun pointing attitude was achieved and the deployment transients had settled, GN&C engineers detected a slow system momentum increase tracked down to a phasing error on the MTBs. Since both ATBs showed similar readings for this issue, a new alignment table was uploaded to the spacecraft for correction. This anomaly is described in detail in the 'Flight Anomaly 2' section below.

At GMT 058/22:15, ST-A was powered on for checkout and performance of the ST was verified. The HGA deployment process started at GMT 059/01:04, approximately 2 hours later. This deployment involved the antenna folding out from the stowed launch configuration and locking into its final position for the duration of the mission. GN&C engineers were able to verify HGA deployment and locking by looking at the spacecraft system momentum response at GMT

059/01:16. Following the verification of ST-A, ST-B was powered on at GMT 059/01:50 for verification. After performance of ST-B was verified, both STs were left in a powered state. Though only one ST is used for spacecraft control, both STs are left powered in order to have a hot backup and to monitor the health and performance of the backup ST.

The GPS Navigators (Nav-A and Nav-B) were the next GN&C hardware to be tested on-board. Nav-B was powered on first, at GMT 059/02:14, and Nav-A was powered on 4 minutes later. The objective was to gather at least 1 orbit of parallel data in order to verify the solutions and monitor time data for both navigators. The Navigators produced both point solutions and filtered solutions using the Goddard-developed GPS-Enhanced Onboard Navigation System (GEONS) filter. Solutions from each Navigator were compared to each other and to ground determined solutions. Upon initiation, a valid point solution from each navigator was successfully detected from the very first telemetry point. Both Navigators showed consistent readings at initial powering. The point solutions were within 5m position and 5cm/s velocity for the two receivers. The GEONS[3] filtered solutions were within 5m position and 1cm/s velocity. Both GPS receivers were kept on for a day and a half at the request of the Navigator hardware lead, in order to get as much data as possible before GPS-B was turned off for the duration of the nominal mission. The only Navigator related constraint was that one receiver had to be off prior to initiation of the DPR instrument, so this data collection did not disrupt any nominal path forward. Following checkout of the Navigators, GPS-B was powered off. This concluded the powering and verification of all GN&C hardware components.

GPM successfully completed initial checkout activities at GMT 059/06:00. At GMT 059/12:25, once the spacecraft was deemed safe for geodetic nadir pointing, the command to slew to MSM was sent. Once in MSM, verification and calibration of science functions, including DPR offset calibration and GMI deep space calibration, could begin. Shortly after entering MSM, the spacecraft was autonomously sent back to SPM due to an FDC flag. The FDC failure was determined to be a result of high albedo influencing the hardware determined sun vector, and is described in detail in the ‘Flight Anomaly 3’ section below. After engineers determined the reason this flag tripped, the decision was made to passivate the corrective actions following the FDC detection until further information could be collected.

On GMT 068, 10 days after liftoff, another FDC detected Kalman Filter (KF) error nearly sent the Observatory to SPM again. This anomaly, discussed in the ‘Flight Anomaly 4’ section below, was linked to an error in the Flight Software only seen after ST occultation. Once this anomaly was understood, the spacecraft was sent back to MSM and workarounds were put in place to compensate for the FSW error until the flight code could be corrected.

Overall, the GN&C subsystem performed well during the first few days of the mission. The anomalies mentioned above are described in further detail in the subsequent sections.

Flight Anomaly 1: Solar Array Deployment Dynamics

The first unexpected activity of the launch sequence occurred shortly after separation from the launch vehicle. At approximately 10 minutes after positive separation indication, the two solar arrays were set to autonomously deploy. GPM used non-explosive actuators for release of the array launch restraints and deployment of the arrays. The sequence began as expected, and the array deployment itself completed with no issues. However, the on-board FDC software detected a rapid increase in the total system angular momentum and took actions to ensure the safety of the spacecraft.

The FDC check on delta system momentum is primarily meant to detect propulsion system failures. The check trips a software flag if the change in system momentum is higher than 5 Nms

for 3 consecutive software cycles. It has a quick response time (<500ms, nominally) in order to detect and correct accelerations due to inadvertent thruster pulsing. Upon detection of an anomalous angular acceleration, the system closes all propulsion latch valves and sends the spacecraft to its sun-pointing orientation in SPM.

During the Launch and Early Operations sequence, real-time telemetry is limited due to the available bandwidth of the S-band link. On-board telemetry is also down-sampled to once per 10 seconds in order to conserve data storage space. This telemetry sampling made reconstruction of the events surrounding the FDC actions difficult. However, enough data was collected to show substantial change in system momentum had occurred (Figure 2). Large jumps in the estimated system momentum occurred at approximately Sep+610 seconds and Sep+655 seconds. From the event log, it was during the second of these two events that the FDC check failed. It cannot be seen from the down-sampled, on-board storage data whether there was sufficient change over three 10Hz cycles to warrant the actions, but there is enough circumstantial evidence to conclude that the system responded to the unexpected large torques on the body due to the solar array deployment.

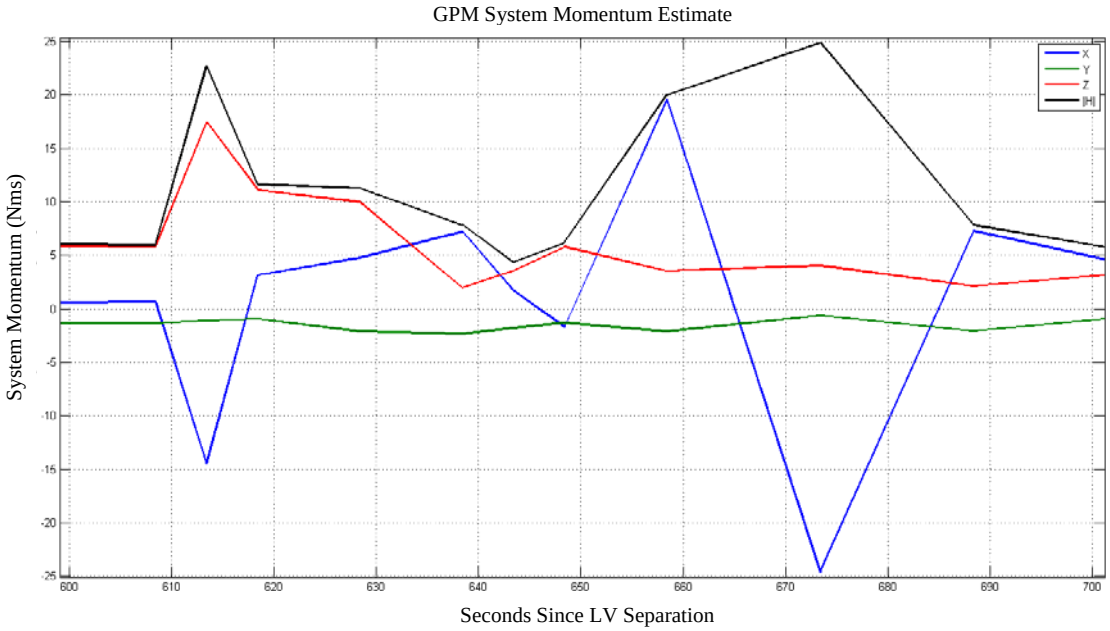

Figure 2: System Momentum Estimate During Solar Array Deployment.

In this instance, the GPM spacecraft was already configured for nominal Safehold, acquiring the sun, and had the latch valves closed, so fewer actions were actually taken by the on-board software. In particular, the B-side CSSs, MSSs, and MTBs were selected for use. Some minimal effort was needed to put the system back into its nominal post-launch configuration and continue checkout activities.

In retrospect, more analysis could have been done on the actual solar array deployment and the dynamic interaction with the GPM core body. Also, the FDC check on delta system momentum could have been disabled until after solar array deployment. Given the resources needed for the dynamic analysis, and the low risk of propulsion issues prior to propulsion system checkout, the latter would have likely been the recommended choice.

Flight Anomaly 2: Angular Momentum Build-up

After the transients of separation from the launch vehicle, initial deployments, and Sun acquisition had settled, the GN&C engineers on console in the GPM launch support room observed that the observatory system momentum was slowly increasing (Figure 3). Although limited real-time telemetry was available and the spacecraft dynamics were not yet quiescent, the experience of the engineers on console with simulations and performance testing led to additional scrutiny of the trend. At this point, less than one full orbit's worth of data had been collected and the existence of an anomaly was not a certainty. However, the GPM Systems Engineering team was notified immediately of the concern and the decision was made to continue monitoring the data trend and consult the contingency documentation to eliminate potential sources of the issue.

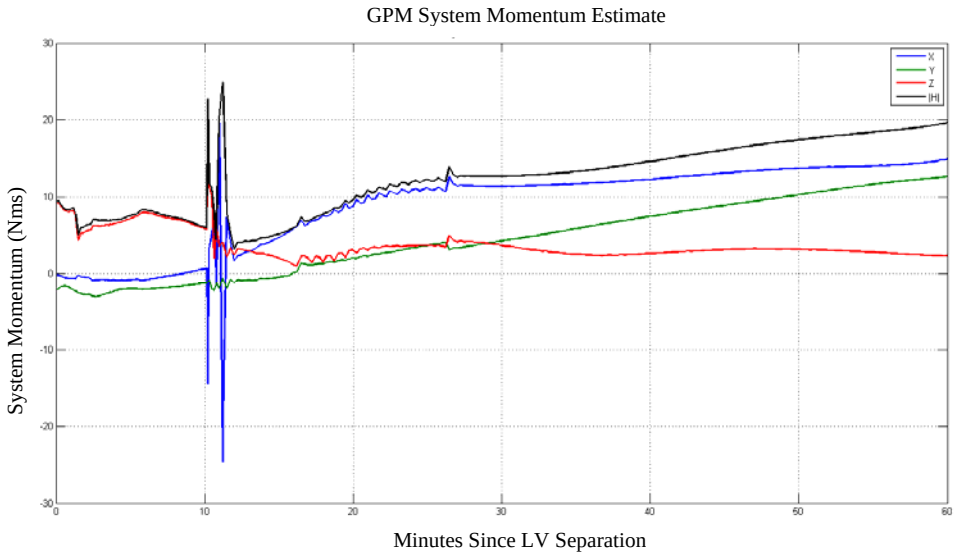

Figure 3: System Momentum Trend During First Hour.

The decision to wait and monitor was based on several factors. First, the cyclic nature of disturbance torque from aerodynamic drag for an inertial pointing spacecraft induces that same kind of cyclic response in the system momentum. In addition, the low bandwidth momentum management controller cannot completely compensate for this effect using the MTBs due to the physical constraints of Earth's magnetic field, and tends to induce a parasitic momentum effect that is orbital in period. Lastly, the current system momentum levels were less than 10% of the capability of the 5 reaction wheels.

The engineering team consulted the contingency flows to verify their initial supposition: the polarity of the MTBs was reversed. Data from the SIRU, magnetometers, and reaction wheels were revisited to verify their proper performance. Also, some consideration was given to the possibility that only one or two of the three bars had its polarity reversed, but the indication from the data and the review of the ground test program gave confidence that the issue was with all three MTBs. Approximately 90 minutes into the mission, an anomaly was declared and the MTB current drive was overridden to zero while new software tables were being prepared for upload. Once the MTB current was overridden, the rate of momentum growth noticeably decreased, giving the engineers on console more confidence of the source of the problem.

A new flight software table was generated that negated the orientation of the MTB axes in the body frame. Care was taken to ensure the validity of the table prior to the upload and after the load

was complete. The upload sequence took about 20 minutes and 6 hours and 5 minutes after separation from the launch vehicle, the new tables took effect. Within 30 minutes, the total system momentum had decreased by 30%. Nominal momentum levels were reached less than an orbit after the new tables took effect. The new tables were burned into EEPROM on both processor sides so that any further entry into Safehold would be in the correct momentum management configuration, allowing for fault tolerance.

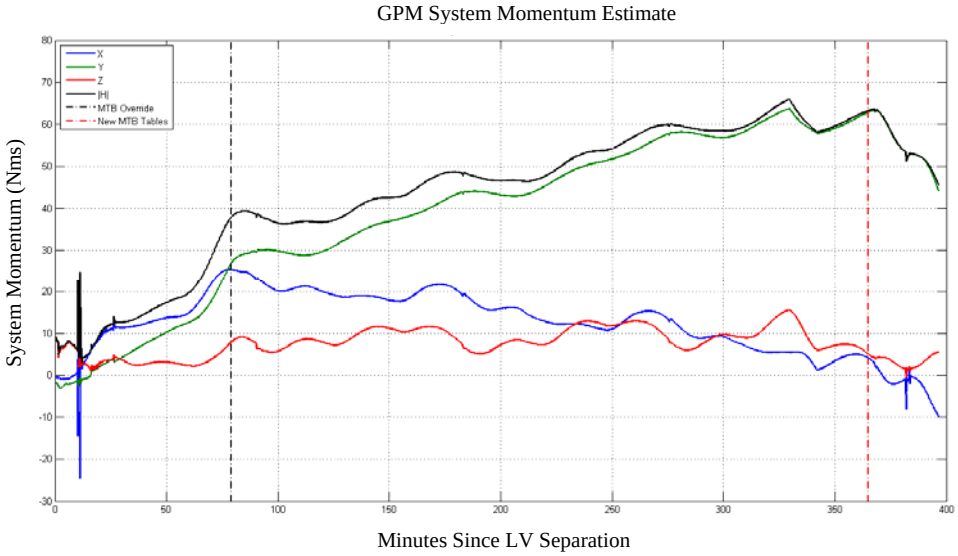

Figure 4: System Momentum Trend During MTB Anomaly.

After GPM commissioning activities were concluded, an investigation into the cause of the phasing issue was conducted. This investigation looked into the vendor documentation, test equipment, and testing documentation. Ultimately, it was determined that the anomaly occurred because of both incorrect assumptions about the field direction as stated in the MTB documentation and an incorrect understanding of the ground test magnetometer instrument. The test campaign should have caught the issues, but the test was not properly set-up to distinguish phasing errors in the spacecraft body axes. Also, the same team that defined the test approach was also the team who reviewed the results of the phasing tests. Any incorrect assumptions that went into designing the test were also used in determining the success criteria. No external project review of the phasing test procedures and results was conducted, which likely would have flagged the approach as a potential issue.

Flight Anomaly 3: Sun Vector Discrepancy

Shortly after entering MSM using a nadir tracking target, the spacecraft unexpectedly went into Safehold due to one of the autonomous FDC tests. The test that failed compares the Sun vector calculated using the CSSs against the Sun vector calculated using the on-board models (OM) Sun vector and estimated attitude from the KF. This particular test is intended to be a “last resort” comparison between the very basic CSS Sun vector estimate and the State Determination (SD) Sun vector that relies on the SSIRU and ST. The original test criteria was that the angular error between the two Sun vectors had to exceed 20 degrees for 2 minutes. Albedo was expected to be a potential issue for the CSS estimated Sun vector, but it was thought that a 20 degree limit for 2 minutes would not be exceeded erroneously.

Once the spacecraft was safely pointed on the Sun line in SPM, the GN&C engineers checked out the hardware and confirmed that everything was performing nominally. No other FDCs had failed and the STs, SSIRU, and CSSs were all functioning as expected. The decision was made to passivate that particular FDC, transition the spacecraft back to MSM, and continue with the investigation as to why that particular FDC failed. With the FDC in passive mode, as opposed to being disabled, event messages would still be sent when FDC limits were exceeded. Once back in MSM and nadir tracking, it was observed that that particular FDC continued to exceed limits every orbit around the same point in the orbit ground track. As can be seen in Figure 5, the Sun angle error FDC was tripping right above the coast of Antarctica. The premise was then that the reflection of the Sun on the snow and ice was causing the CSS Sun vector to have a larger error.

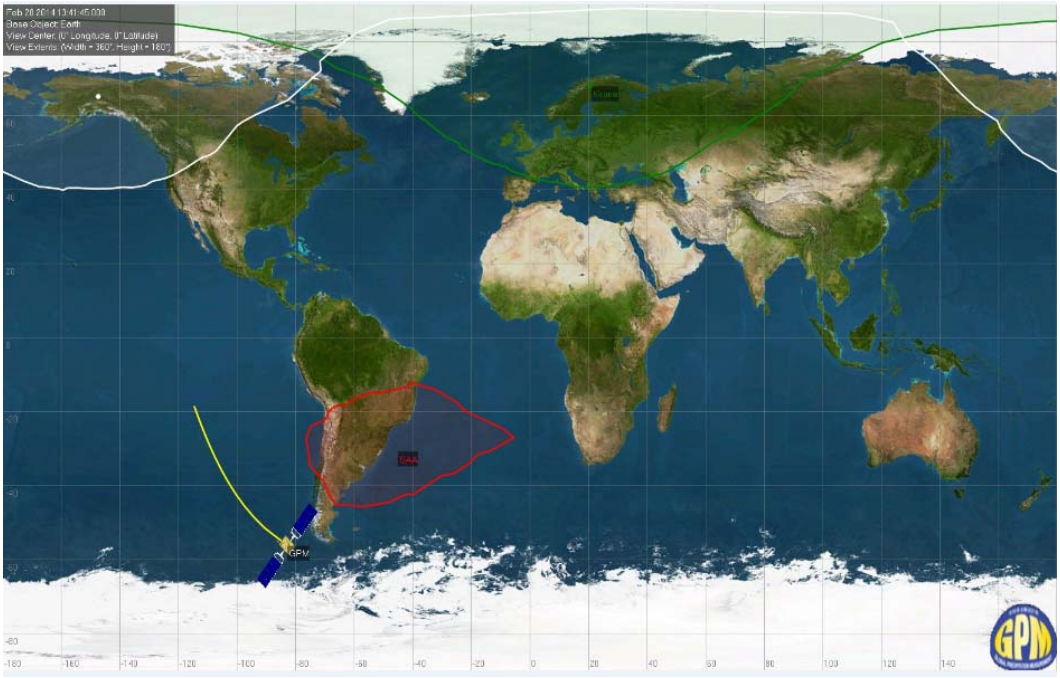

Figure 5: GPM Ground Track Map at Time of CSS Sun Vector FDC Trip.

Figure 6, shows the angular error between the CSS Sun vector and the SD/OM Sun vector for one day's worth of orbits. As can be seen in the Figure, the FDC limit was being exceeded almost every orbit. As designed, the FDC test was not going to work effectively. New limits and persistence would have to be established prior to enabling that particular FDC again. Because the GN&C team also believed that the error could also be dependent on Beta angle and season, it was decided to collect data for a long period of time prior to selecting new limits.

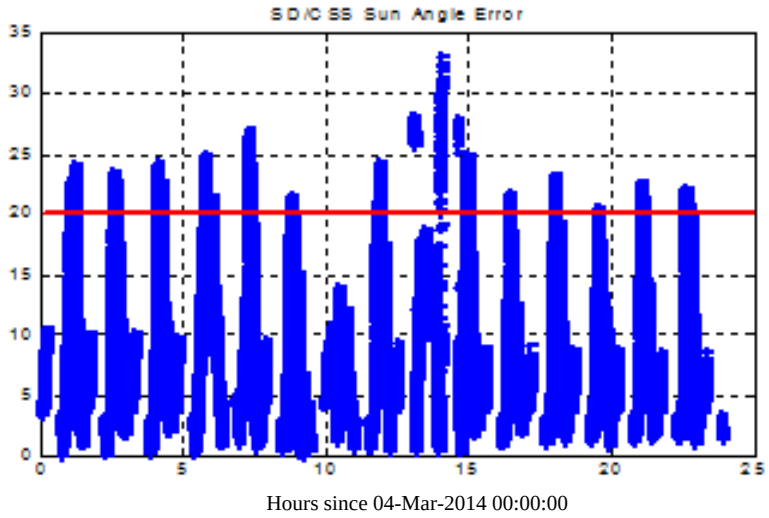

Figure 6: State Determination/CSS Sun Angle Error.

Using data collected over several months, the GN&C team suggested increasing the angular error limit to 30 degrees and the persistence to 5 minutes. Even though angular errors greater than 30 degrees had been seen, it was felt that increasing the limit more than that would effectively disable the FDC check entirely. It was believed that increasing the persistence to 5 minutes would account for potential exceedences. These changes were implemented shortly thereafter, but, since there were other FDCs in place to monitor the performance of the State Determination, it was decided to leave the Sun Vector FDC in passive mode for a while longer to monitor the new limit and persistence. At this point in time, the FDC is still in passive mode.

Flight Anomaly 4: Delta Quaternion

On March 9, 2014 (Day of Year 068), the GPM Core Observatory entered a period in which the ST was being occulted by the moon every orbit. This type of occultation results in the ST falling out of its tracking mode. The on-board FDC would then automatically promote it back to tracking mode following the end of the computed occultation period. Upon reacquisition of ST data each orbit, one of the KF related APs tripped. The fault that tripped was AP-86, the ST-KF Adjusted Residual Error check. This particular check compares the delta quaternion between the gyro-propagated attitude solution and the ST-based attitude solution against a limit. This delta quaternion would normally be expected to be near zero, even after a lunar occultation.

Tripping of this AP with 60-second persistence had two effects. It reset the KF, and activated AP-87, which provided a second tier of response to KF failures. In the event of further KF FDC failures, if AP-87 was tripped one of the results would be for the spacecraft to transition to SPM. This configuration was meant to guard against persistent KF problems, but because lunar occultations would be occurring every orbit for a number of days, the same fault that tripped AP-86 would trip AP-87 the next orbit if left active, causing an unnecessary transition to SPM. For the first several orbits, AP-86 and AP-87 were manually managed by disabling the active AP, and resetting and re-enabling the other. Managing these APs every orbit became operationally cumbersome, so an alternative solution was desired.

As a stop gap to determining the cause of the apparent large KF residuals and to avoid an undesired and unnecessary transition to SPM, the RTS used to re-promote the ST back to its tracking mode was augmented so that 10 seconds after the ST is re-promoted to tracking mode, the KF is

reset, restoring small residual values before the 60-second limit that would cause AP-86 to trip and activate AP-87.

Once the operational workaround was implemented, further investigation into the root cause of the FDC failure continued. The problem was tracked down to a combination of the calculation of the delta quaternion between the ST measurement and the SIRU propagated solution and the fact that the ST generated attitude quaternion always selects a positive fourth component upon entering its tracking mode.

A given Earth Centered Inertial (ECI)-to-device attitude (the device being either ST or spacecraft in this context) can be represented in quaternion form as one of two rotations, one in the range $[0, \pi]$, and the other in the range $[\pi, 2\pi]$ in the opposite direction. The ST, when promoted to tracking mode, selects the first convention for representing its attitude solution. As long as the ST remains in tracking mode, subsequent cycle-to-cycle solutions are selected to have the minimum apparent angular change from the previous solution. Since GPM has a continuous 1-Rotation per Orbit motion when nadir tracking, this convention, combined with the nature of quaternion mathematics, results in a smooth variation of the ST quaternion components over a two-orbit period, with one orbit having the $[0, \pi]$ convention, and the next having the $[\pi, 2\pi]$ convention.

Figures 7 and 8 show plots of the fourth component of the ECI-to-ST and ST-based ECI-to-spacecraft quaternions over a 12 hour period that includes four orbits preceding the lunar occultations of March 2014 and four orbits that include occultations. Note the 2-hour quaternion periodicity when there is no ST reset and the once-per-orbit ST phase reset to positive fourth component with the occultations. The ST-based ECI-to-S/C phase jump occurs when the ST returns to track mode.

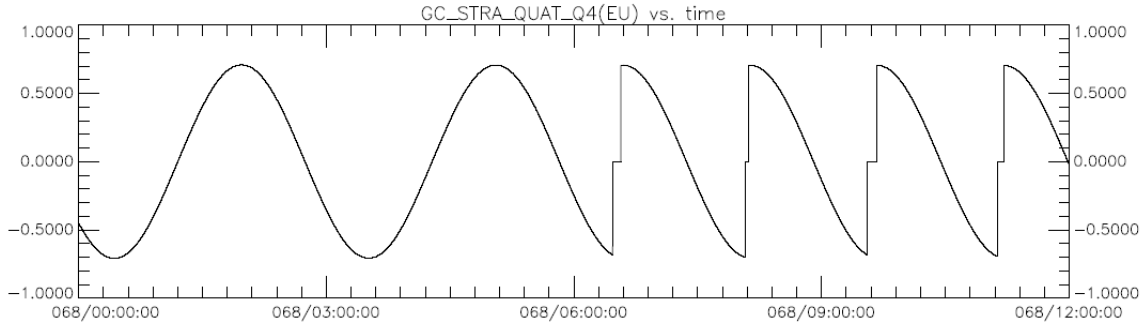

Figure 7: ST-A quaternion fourth component

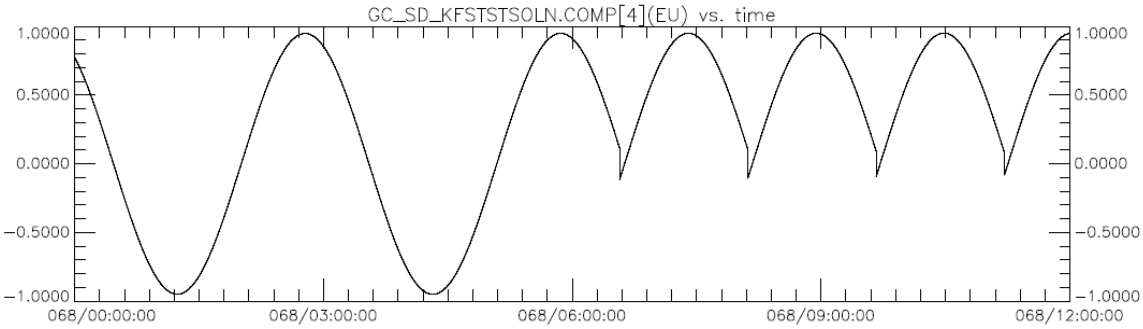

Figure 8: ST-based ECI-to-S/C quaternion fourth component

Figure 9 shows a plot of the fourth component of the gyro propagated ECI-to-spacecraft quaternion over the same 12 hour period. Note that there are also phase jumps in this quaternion, however those phase jumps coincide with when the KF was reset. Upon reception of a KF enable command, the KF synchronizes its ECI-to-spacecraft rotation convention based on that of the ST. This solution is propagated forward, cycle-to-cycle, using gyro data and will follow the same two-orbit periodicity in solution convention described above. So long as the ST remains in track mode, the new ST-based solution and the gyro-propagated solution will remain phase locked with respect to solution convention and the estimated attitude difference between the two will remain small (on the order of ST noise).

However, whenever the ST falls out of track mode and then is re-promoted to track mode, the solution will start in the [0, π] phase. If this happens to not be the phase that would have pertained if the ST mode had not cycled, the ST-based ECI-to-spacecraft attitude solution and the gyro-propagated attitude solution will be 2π out of phase with each other. Recall that the FDC check that failed was the error between the ST-based ECI to spacecraft attitude solution and the gyro propagated attitude solution. Typically, when such delta quaternions are calculated, the fourth component of the quaternion is forced to have a positive value, thus ensuring the calculation is close to zero.

Further investigation into the Flight Software calculation of the delta quaternion calculation revealed that it was not enforcing a positive fourth component after the delta quaternion was calculated and therefore the resulting quaternion error was seen to be close to 2π, rather than close to 0. Resetting the KF causes the KF attitude solution, and the gyro-propagation thereof, to resynchronize with the phase of the ST-based ECI-to-S/C attitude solution, thus restoring the difference between the two solutions to be near 0.

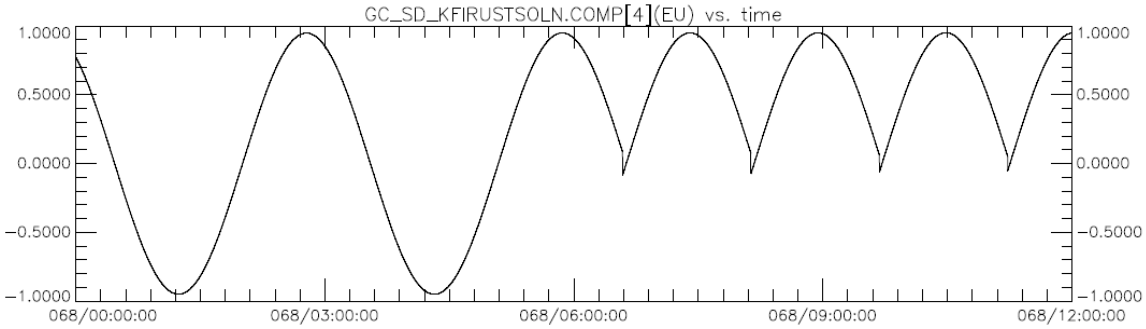

Figure 9: Gyro-propagated ECI-to-S/C quaternion fourth

A solution to the problem was determined to be a repair in the FSW by forcing the use of the [0, π] phase convention on the delta-quaternion, residual rotation (i.e., force a non-negative fourth component of the delta quaternion) between ST-based attitude and the gyro propagated attitude in the KF utility code. This FSW update was thoroughly evaluated for spacecraft affects before being uploaded to the satellite.

CONCLUSION

On May 29, 2014, the GPM Core Observatory was successfully handed over to the Mission Flight Operations Team at GSFC in Greenbelt Maryland. No mission is without its surprises, but the GN&C team was able to look at the behavior of the spacecraft and identify where the potential spacecraft or hardware issues were. The attention and dedication of the GPM team enabled all anomalies to be mitigated in a timely manner before any additional issues were realized. This paper

described the importance of paying close attention to the minor details. It is these details that can potentially compound and cause issues for the spacecraft.

Ten days after launch, GPM was able to capture first of its kind images of precipitation inside a cyclone over the North West Pacific Ocean. Following several instrument calibrations and verifications, GPM released its first public data set in June, 2014. It is currently on orbit, collecting meaningful scientific data.

ACKNOWLEDGMENTS

We'd like to acknowledge the substantial efforts of many colleagues in the development and implementation of the GPM GN&C algorithms. Besides ourselves, the following attitude control system analysts also worked on the development of the algorithms over the years: Kuo-Chia (Alice) Liu, Scott Heatwole, Kong Ha, Carl Blaurock, Kristin Bourkland, and Henry Fitzpatrick. The following members of the GPM GN&C flight software development and test teams implemented and verified the algorithms within the flight system (with significant feedback that helped improve the algorithms): Ji-Wei Wu, Michael Yang, David Hardison, Bruce Trout, David Kobe, Maureen Bartholomew, Jack Fu, Anren Hu, Alexander Calder, William Keksz, Michael Lambertson, Steve Judy, and Jacob Rosenberg. Simulation system support was provided by Steven Queen, John Vaneepoel, Stephen Leake, and Steven Messiora, and GN&C systems support by Tim Gruner.

REFERENCES

[1] Fitzpatrick, Henry, and DeWeese, Keith, "Safehold Attitude Determination Approach for GPM," Advances in the Astronautical Sciences 144 (2012): 213-222.

[2] Winternitz, Luke, Moreau, Michael, Boegner, Jr., Gregory J., and Sirotzky, Steve, "Navigator GPS Receiver for Fast Acquisition and Weak Signal Space Applications," presented at ION GNSS, Long Beach, CA (2004).

[3] "GEONS Open Architecture Solutions for Onboard Orbit Determination in any Orbit," Goddard Space Flight Center, Mission Engineering Systems Analysis Division, http://geons.gsfc.nasa.gov.